Freeze-Thaw Behavior of FRP-Confined Concrete under Sustained Load

by A. Kong, A. Fam, and M.F. Green

Synopsis: Fiber-reinforced polymers (FRPs) are effective in strengthening concrete structures. However, little work has examined the effects of cold regions on the behavior of the strengthened members, particularly the combined effects of sustained loading and freeze-thaw exposure. This paper presents the results of an experimental study on the durability of 70 normal weight, low strength, and non-air entrained concrete cylinders (150 x 300mm). The cylinders were confined with glass-FRP (GFRP) sheets or carbon-FRP (CFRP) sheets and exposed to 300 freeze-thaw cycles while under sustained axial compression loads. FRP-wrapped cylinders showed exceptional durability performance after their extreme exposure to freeze-thaw and sustained loading with a maximum of 12% reduction in strength. Some CFRP wrapped cylinders that were exposed to freeze-thaw without longitudinal restraint, by means of sustained loads, and all the plain concrete cylinders were completely disintegrated with virtually zero residual strength.

Keywords: concrete; confinement; creep; durability; fiber reinforced polymer (FRP); freeze-thaw; sustained load; wraps

Andrew Kong is currently a Masters Student in the Department of Civil Engineering at Queen's University at Kingston, Ontario, Canada. He received a B.Sc. from North Carolina A&T State University, U.S.A., 2002. Current research involves creep and durability of fiber reinforced polymer (FRP) used as external reinforcement for concrete cylinders.

ACI member **Amir Fam** is an Assistant Professor and Canada Research Chair in Innovative and Retrofitted Structures at Queen's University, Canada. He is a voting member of ACI Committee 440, FRP Reinforcement and a Co-Chairman of Sub-Committee 440-J, FRP Stay-in-Place Formwork. His research includes applications of FRP in new construction and retrofit of existing structures.

ACI member **Mark F. Green** is a Professor in the Department of Civil Engineering at Queen's University at Kingston, Canada. He received his Ph.D. in Engineering from Cambridge University, UK, in 1991. He is an active member of ACI committee 440 Fiber Reinforced Polymer. His research interests include strengthening concrete structures with FRPs, prestressing concrete beams with FRPs, and bridge-vehicle dynamics.

INTRODUCTION

There has been an ever-increasing need for structural repair of existing infrastructure that is now rapidly deteriorating. Over the past fifteen years, engineers and material scientists have made great strides by incorporating Fiber Reinforced Polymer (FRP) composite materials into design and construction to meet this need. These materials have been successful in many applications, but little information is available on their behavior in cold regions. In particular, the combined effects of sustained loads and freeze-thaw exposure have not been studied by researchers (Karbhari et al. 2003).

One application of FRPs is to confine concrete columns to increase their axial strength and ductility. In cold climates, these columns will be exposed to low temperature, and freeze-thaw action. FRP composites exposed to freezing temperatures and alkaline solutions may suffer matrix microcracking, degradation in the fiber-matrix bond, and even damage to the fibers themselves (Karbhari et al. 2000). Some researchers have examined confined concrete cylinders exposed to freeze-thaw or to sustained loading, independently. Karbhari and Eckel (1993) tested FRP wrapped cylinders at low temperature (-18°C), and found increased brittleness of FRP fibres at low temperature. Soudki and Green (1996) found good performance of carbon FRP strengthened columns when subjected to up to 200 freeze-thaw cycles consisting of 16 hours of freezing in air (-18°C), followed by 8 hours of thawing in a water bath (+15°C). Toutanji and Balaguru (1998) exposed FRP wrapped concrete cylinders to 300 freeze-thaw cycles and found slight deterioration due to freeze-thaw cycles, with carbon FRPs performing better than glass FRPs.

Other researchers have studied the creep behavior of FRP-wrapped cylinders under sustained axial loads. However, no research has been reported on FRP-wrapped cylinders subjected to the two conditions combined, as in actual structures, which may have a synergetic effect. Creep in polymers is commonly known as viscoelastic deformation, which is a combination of elastic deformation and viscous flow (Mallick 1988). Stress level and temperature are two factors that influence creep-strain in composites. Orientation of the fibers is another factor that needs to be considered when analyzing creep in polymers. If the main fibers are in the direction of the load, then the composite creep is dependent on creep in the fibers. Studies of creep were conducted by Naguib and Mirmiran (2002) on concrete-filled FRP tubes showed that shrinkage and creep of concrete in this case is much lower than exposed concrete due to the sealing effect.

In the research project described in this paper, FRP-wrapped concrete cylinders (152 x 305 mm) have been subjected to 300 freeze-thaw cycles, while simultaneously being subjected to sustained axial compression loads. This small size of specimen was selected for ease in repeating the results on many specimens, and so that the capacity of testing machines at Queen's University was not exceeded. Further, most tests in the literature on FRP wrapped concrete cylinders have been conducted with this size of specimen (Bisby et al. 2005). Tests on larger-scale specimens should be conducted to better understand the behavior of full-scale columns in the field. The concrete was not air entrained to simulate the worst-case scenario for concrete. Thus, better freeze-thaw resistance is expected for concrete with appropriate air entrainment. Test results of specimens subjected to the combined effects have been compared to those of other specimens subjected to sustained loading at room temperature and to those of specimens subjected to freeze-thaw without sustained loading. Two numerical models, one developed by ISIS Canada (ISIS, 2001), and the other developed by ACI Committee 440 (ACI 2001) were also used to compare the predicted confined strength of the control cylinders at room temperature with the experimental data.

RESEARCH SIGNIFICANCE

Durability of FRP-retrofitted concrete structures is a major concern. Research conducted on durability of FRP-confined concrete cylinders has concentrated on the effect of harsh environments but without the effect of sustained loads. By applying sustained loads to FRP-wrapped cylinders, the effect of freeze-thaw cycles may be more critical due to the development of internal micro cracks in the concrete under the loads. This paper discusses experimental results examining the freeze-thaw durability of FRP-wrapped cylinders while under sustained loads. The results will provide valuable data for design procedures and for engineers considering FRP repair of columns in cold climates.

EXPERIMENTAL PROGRAM

Seventy (70) concrete cylinders, (152 mm (6in) in diameter and 305mm (12in) in length) were cast. No air-entrainment was used to simulate a worst-case scenario for concrete in harsh weather conditions. The cylinders were removed from the molds after 7 days and allowed to air cure at room temperature. The cylinders were designed to have a compressive strength of 20 MPa after 28 days; the average tested strength at 28 days was 22 MPa. Low strength concrete was used to simulate strength of concrete in old structures. Two sets of 25 cylinders each were wrapped with one layer of CFRP sheet or with one layer of GFRP sheet. The remaining 20 cylinders were left unconfined and used for verification of concrete strength after the completion of freeze-thaw cycles. The manufacturer's properties of the CFRP and GFRP composites are shown in Table 1. After the wrapped cylinders were fully cured, their ends were carefully ground to achieve a smooth surface perpendicular to the main axis of the cylinder.

Before applying sustained loads and freeze-thaw exposure, all test cylinders were first subjected to one monotonic loading cycle, up to a load level of about 45 percent of their respective ultimate strength, unloaded, and then were submerged in water in room temperature for a week. This practice was adopted to promote the worst possible conditions, where microcracks were induced and the internal moisture content was maximized.

Four loading frames were built with the capability to apply sustained loads of 1200 kN each to a series of 5 concrete cylinders. Each frame consisted of 4 # 27mm B16 threaded rods, 2.7m long, and three 50 mm thick mild steel square plates that were 250 x 250 mm as shown in Figure 1. Two frames were placed in the cold room and the other two were always kept at room temperature, simultaneously. Each frame accommodated 5 cylinders placed concentrically in a series. The two frames in the environmental chamber each had 5 CFRP-wrapped and 5 GFRP-wrapped cylinders (Figure 1(a)). This was also the case for the two frames at room temperature (Figure 1(b)). Fifteen control cylinders (5 with CFRP, 5 with GFRP and 5 unconfined) were also placed in the environmental chamber but without sustained loads. Six control (unconfined) cylinders were left at room temperature to determine any increase in concrete strength due to aging by the end of testing period. Three of the six cylinders were submerged in water for a period equivalent to the total number of thawing hours to simulate the curing effect during water-thawing in the environmental chamber, while the other three were kept dry.

A few cylinders were cast with thermocouples inside the concrete core, to measure the concrete core temperature, to help determine the appropriate program to be used for controlling the environmental chamber (cold room), according to ASTM C666 (Standard Test Method for Resistance of Concrete to Rapid Freezing and Thawing) (ASTM 1997). All test specimens were subjected to 300 freeze-thaw cycles, with the temperature of the concrete core varying from +4.4˚C to -18˚C in 5 hours and 15 minutes (Figure 2). The cycles were very repeatable due to the excellent control of temperature available in the chamber. Since no standard exists for FRP-wrapped concrete cylinders, the standard for plain concrete cylinders was employed.

The sustained load was applied to the cylinders in the frame via a 979 kN hydraulic ram. To measure and monitor the sustained load, a 445 kN load cell was fitted in the frame to continuously monitor the load. This load was maintained constant, using the hydraulic ram throughout the duration of freeze-thaw for both the frames inside and outside the cold room. After the completion of the 300 freeze-thaw cycles, all cylinders were tested under axial compression, using a 1000 kN MTS machine. Each cylinder was instrumented with three 100 mm displacement based strain gauge transducers spaced around the perimeter to measure axial strains, and two 5 mm electric resistance strain gauges to measure hoop strains on two opposite sides of each cylinder.

TEST RESULTS AND DISCUSSION

Test results, in terms of axial compressive strength and ultimate axial and hoop strains are reported in Tables 2 and 3 for CFRP-wrapped and GFRP-wrapped cylinders, respectively. In each table, results are given for both specimens subjected to freeze-thaw cycles and those kept at room temperature, with and without sustained loading for each case. Table 4 shows the test results of plain concrete cylinders at room temperature for both the water cured cylinders and the dry cylinders. For each parameter that was varied, 3 or 4 specimens were tested. All of the results are presented in Tables 2 to 4 and the tests were very repeatable. The specimens are labeled with a 3 letter code; the first letter indicates the type of wrap (C-carbon, G-glass, U-none), the second letter indicates the environmental exposure (F-freeze-thaw, R-room temperature), and the third indicates the type of loading (S-sustained load, C-control with no load). It should be noted that all the five unconfined cylinders placed in the water bath in the environmental chamber were completely disintegrated due to freeze-thaw damage with virtually zero residual strength. Careful observation during freeze-thaw cycling revealed that, at 35 cycles, these unconfined cylinders developed major cracks, and at 100 cycles, they were completely disintegrated, as shown in Figure 3(a). All the unconfined cylinders at room temperature were tested and the ones that simulated the wet-dry condition, occurring in cold room, showed a 4% increase in strength over the ones that were kept dry (Table 4).

The average strength of the CFRP-wrapped cylinders was 40 MPa, which represented a 91% strength increase over the strength of the unconfined cylinders (22 MPa). Three of the four CFRP-wrapped control cylinders (without sustained loading) were completely damaged during freeze-thaw cycling, as shown in Figure 3(b), and were not tested in axial compression. This was attributed to expansion of the concrete core in the longitudinal direction, which was not uniform and resulted in bending of the cylinders. Because all the fibers in the CFRP sheet were oriented in the hoop direction, expansion was not restricted longitudinally. At the overlap location, however, the wrap was slightly stiffer longitudinally due to more fibers and epoxy at this location. Thus, less expansion occurred at the location of the overlap, causing bending. Only one CFRP-wrapped control cylinder could be tested after the completion of the 300 freeze-thaw cycles; this cylinder had a strength of 34.6 MPa.

Also, one CFRP-wrapped cylinder failed under sustained load while undergoing freeze-thaw cycles. Without including this one result, Table 2 shows that freeze-thaw caused only a 3% strength reduction for specimens under sustained loads (CFS vs. CRS Specimens). For the one specimen that survived the freeze-thaw without sustained load, the strength reduction was 12 % (CFC vs. CRC Specimens). Since the other 3 specimens did not maintain integrity for the full duration of the freeze-thaw, the effect of freeze-thaw without sustained loading could be larger than a 12% reduction. It also appears that sustained loading increases the strength by about 7 % at room temperature.

The average strength of the GFRP-wrapped cylinders was 38 MPa which represented an 81% increase over the unconfined cylinders. Results in Table 3 indicate that freeze-thaw caused only a 3% average reduction in strength for specimens under sustained loads

(GFS vs. GRS Specimens) and a 6 % reduction for specimens without sustained loading (GFC vs. GRC Specimens). This confirms quite well the observations on the CFRP-wrapped cylinders. It was also noted that sustained loading had almost no effect on strength in this case (GRC vs. GRS and GFC vs. GFS Specimens).

Figures 4 to 8 show the stress-strain curves for the plain concrete cylinders, the CFRP-wrapped, and the GFRP-wrapped cylinders. Each graph shows the stress versus average axial and hoop strains. The plain concrete cylinders were severely damaged due to freeze-thaw only (no sustained load) because of the lack of air-entrainment. These specimens were completely disintegrated, and could not be tested. As such, Figure 4 shows the behavior of plain concrete cylinders at room temperature only. On the other hand, the confined concrete, after 300 freeze-thaw cycles, maintained approximately the same strength as the control specimens (Tables 2 and 3). Thus, the FRP-wrapping performed exceptionally well except in the case of the CFRP-wrapping without sustained load.

The cylinders that were subjected to sustained load, at both room temperature and freeze-thaw, showed a distinctly different behavior from those not subjected to sustained loading. For example, in Figures 6 and 8, the specimens that were not subjected to sustained load (CRC and GRC) started the transition in the bilinear behavior at a lower load than for the sustained loaded specimens (CRS and GRS). This change in the transition load is attributed to creep which causes axial strains to increase under constant stress. Consequently, the radial and hoop strains will also increase due to Poisson’s ratio (dilation) effect. This mechanism activates the confinement imposed by the FRP jacket. At the end of sustained loading, residual strains remain due to material non-linearity (i.e., plastic flow due to creep effects). Thus, the sustained loading appears to create a state of active confinement. Further research may be needed to confirm this hypothesis. The fact that the axial and hoop strains at failure are lower for the specimens under sustained loads gives some credence to this hypothesis. It should be noted that such a state of active confinement would not be expected in a field repair since the sustained loads in the field would be present at the time of wrapping and most of the creep would have occurred before wrapping. Thus, the state of active confinement may not occur in practice.

From the overall results, the GFRP-wrapped cylinders resisted freeze-thaw effects better than the CFRP-wrapped cylinders. Two potential mechanisms for the better performance of the GFRP were identified. The first relates to the amount of epoxy used for the two different materials. Although a similar amount of epoxy was used for each type of FRP, the GFRP appeared to absorb more epoxy. Thus, the protection for the GFRP wrapped cylinders may be due to the adherence of more epoxy. Alternatively, the CFRP sheets had all the structural fibers running in the hoop direction and no fibers in the axial direction, whereas the GFRP had most of the fibers (more than 90%) in the hoop direction but had some aramid fibers in the axial direction. These longitudinal aramid fibers may have helped the GFRP-wrapped cylinders resist the axial expansion and contraction of the concrete core during freeze-thaw cycling.

The test results were obtained for small-scale cylinders under purely axial compressive load. Thus, tests on larger specimens and/or with eccentric loading would be useful to continue this work to better represent conditions in the field.

Failures Modes

The mode of failure was governed by tensile fracture of the FRP sheets in the hoop direction. After the hoop stresses induced by the confinement pressure exceeded the FRP tensile capacity, loud popping sounds were heard. At this point, the system was unable to withstand further loading and the specimen failed, as shown in Figure 9. The majority of cylinders failed by fiber rupture at the mid-height of the cylinder. The stress-strain curves clearly demonstrated that the FRP-confined concrete cylinders exhibited a bilinear response with no descending branch. GFRP-wrapped cylinders subjected to freeze-thaw without sustained load had the quietest and least dramatic failure mode, whereas CFRP-wrapped cylinders subjected to both freeze-thaw and sustained loading had the loudest and most catastrophic failure mode.

NUMERICAL MODEL

The following models developed by ISIS Canada (ISIS 2001), and ACI Committee 440 (ACI 2001), were used to predict the FRP-confined strength, f_{cc}' of control (room temperature) specimens:

Model 1 (ACI 440)

$$f_{cc}' = f_c'[2.25\{1+7.9(f_l / f_c')\}^{0.5} - 2(f_l / f_c') - 1.25] \quad (1)$$

$$f_l = [K_a \rho_f f_{fe}]/2 = [K_a \rho_f \varepsilon_{fe} E_f]/2 \quad (2)$$

$$\rho_f = 4nt_f / h \quad (3)$$

$$\varepsilon_{fu} = C_E \varepsilon_{fu}^* \quad (4)$$

$$f_{fu} = C_E f_{fu}^* \quad (5)$$

$$E_f = f_{fu} / \varepsilon_{fu} \quad (6)$$

Model 2 (ISIS Canada)

$$f_{cc}' = f_c'(1 + \alpha_{pc} \varpi_w) \quad (7)$$

$$\varpi_w = 2 f_{lfrp} / \phi_c f_c' \quad (8)$$

$$f_{lfrp} = 2N_b \phi_{frp} f_{frpu} t_{frp} / h_c \quad (9)$$

Tables 5 and 6 show the results for the confinement models compared against the experimental values for the specimens tested at room temperature without sustained loading. Table 7 gives the percentage differences between the experimental results and model predictions. The ISIS equations gave a slightly better prediction than the ACI 440 equations. For CFRP-wrapped cylinders, the differences between the experimental results and the two models were: ISIS – 14 % and ACI 440 – 40 %. For GFRP-cylinders the difference between experimental and the two models were: ISIS – 10% and ACI 440 – 26%. In all cases, the confinement models overestimated the strength of the FRP-confined cylinders and thus the models were not conservative when compared against these test results. Bisby et al. (2005) recently compared the ISIS and ACI confinement models against a much wider database of experimental results and found that the ISIS model was generally conservative but that the ACI model was not.

SUMMARY AND CONCLUSIONS

Overall, FRP-wrapped cylinders displayed excellent resistance to combined freeze-thaw and sustained loading. The average reduction in strength for both GFRP-wrapped and CFRP-wrapped cylinders exposed to freeze-thaw, while under sustained loads, was approximately 3%. With only freeze-thaw exposure (no sustained loading), GFRP wrapped cylinders lost an average of 6% of their confined strength while most of the CFRP-wrapped cylinders lost their structural integrity before the end of the freeze-thaw exposure, due to the excessive expansion and contraction in the longitudinal direction. The specimens subjected to combined freeze-thaw and sustained loads performed better than those under freeze-thaw only, since the sustained loading induced active confinement and end restraints, which prevented longitudinal expansion and contraction. It was also observed that the sustained loading caused a stiffening effect, where the transition in the bilinear stress-strain curves of FRP-confined concrete occurred at a higher load level. Some of these effects of sustained loading may not be evident in the field because columns would typically be wrapped when the sustained loads are acting. The confinement model proposed by ISIS Canada design guide predicted the strength of confined concrete cylinders reasonably well, but that the ACI 440 model was not accurate. More research on larger scale specimens is recommended to better reflect field conditions. Further, this current study only considered the effects of axial compressive loads. Further tests on specimens with eccentric loads would yield an understanding of columns subject to both axial and flexural stresses.

ACKNOWLEDGMENTS

The authors are members of the Intelligent Sensing for Innovative Structures (ISIS Canada) Research Network of Centres of Excellence (NCE). This work has been supported by the NCE and the Natural Sciences and Engineering Research Council (NSERC) of Canada. The authors would also like to thank the technical staff at Queen's University and the Université de Sherbrooke.

NOTATION

C_E = environmental reduction factor
E_f = tensile elastic modulus of FRP
f_l = lateral stress produced by confinement
f_{fe} = effective stress in FRP
f_{fu} = design ultimate tensile strength of FRP
f^*_{fu} = tensile strength of FRP by manufacture

f_{lfrp} = confining pressure due to FRP reinforcement
f_{frpu} = tensile strength of FRP
f'_c = strength of unconfined concrete
f'_{cc} = confining strength of concrete
h = overall thickness of member
h_c = diameter of circular column
k_a = efficiency factor of FRP, (based on shape of section)
N_b = number of layers,
n = no of plies
t_f = nominal thickness of one ply
t_{frp} = thickness of FRP
α_{pc} = performance coefficient of circular column
ε^*_{fu} = ultimate rupture strain of FRP
ρ_f = reinforcement ratio
ϕ_c = resistance factor of concrete
ϕ_{frp} = resistance factor of FRP
ω_w = volumetric ratio of FRP strength to concrete strength

REFERENCES

ACI, 2001, "Guide for the design and construction of externally bonded FRP systems for strengthening concrete structures," American Concrete Institute, Committee 440.

American Society of Testing and Material Standards (ASTM), 1997, "Standard Test Method for Resistance of Concrete to Rapid Freezing and Thawing." C666-97, Annual Book of ASTM Standards, pp. 314-319.

Bisby, L.A., Dent, A.J.S., and Green, M.F. 2005**.** "A Comparison of Models for FRP-Confined Concrete," *ACI Structural Journal*, Vol. 102, No. 1, pp. 62-72.

ISIS 2001, "Strengthening reinforced concrete structures with externally-bonded fiber reinforced polymers," Canadian Network of Centres of Excellence on Intelligent Sensing for Innovative Structures (ISIS), Design Manual No. 4.

Karbhari, V.M., Chin, J.W., Hunston, D., Benmokrane, B., Juska, T., Morgan, R., Lesko, J.J., Sorathia, U., and Reynaud, D. 2003. "Durability Gap Analysis for Fiber-Reinforced Polymer Composites in Civil Infrastructure," *Journal of Composites for Construction*, **7**(3), pp. 238-247.

Karbhari, V.M., and Eckel, D.A. II. 1993. "Effect of a Cold-Regions-Type Climate on the Strengthening Efficiency of Composite Wraps for Columns," Technical Report, University of Delaware Center for Composite Materials, Newark, Delaware, June.

Karbhari, V. M., Rivera, J., and Dutta P. K., 2000, "Effect of short-term freeze-thaw cycling on composite confined concrete," *Journal of Composites for Construction,* ASCE, V. 4, No. 4, pp. 163-217.

Mallick, P. K., 1998, "Fiber-reinforced composites: materials, manufacturing, and design." Marcel Dekker, INC., New York, New York.

Naguib, W., and Mirmiran, A., 2002, "Time-Dependent behavior of fiber-reinforced polymer confined concrete column under axial loads," *ACI Structural Journal*, V.99, No. 2, pp. 142-148.

Soudki, K. A., and Green, M. F., 1996. "Performance of CFRP Retrofitted Concrete Columns at Low Temperatures," 2nd International Conference on Advanced Composite Materials in Bridges and Structures, Montreal, Quebec, 11-14 August, pp. 427-434.

Toutanji, H., and Balaguru, P. 1998. "Durability Characteristics of Concrete Columns Wrapped with FRP Tow Sheets," *ASCE Journal of Materials in Civil Engineering*, 10(1), pp. 52-57.

Table 1—FRP properties as provided by the manufacturers

Properties	Type of FRP sheets	
	GFRP	CFRP
Tensile strength (MPa)	575	991
Elongation at break (%)	2.2	1.26
Tensile modulus (GPa)	26.1	78.6
Laminate thickness (mm)	1.3	0.89

Table 2—Test results of CFRP-wrapped concrete cylinders

FREEZE-THAW									
	Under sustained load					No sustained load			
Specimen code	CFS-1	CFS-2	CFS-3	CFS-4	**Avg.**	CFC-1	CFC-2	CFC3	**Avg.**
Strength (MPa)	40	40.2	44	F.D	**41.4**	34.6	F.D	F.D	**34.6**
Avg. axial strain	0.00927	0.00875	0.00841	0	**0.00898**	0.01329	0	0	**0.01329**
Avg. hoop strain	0.00403	0.00697	0.01127	0	**0.00757**	0.00474	0	0	**0.00474**
ROOM TEMPERATURE									
	Under sustained load					No sustained load			
Specimen Code	CRS-1	CRS-1	CRS-3	CRS-4	**Avg.**	CRC-1	CRC-2	CRC-3	**Avg.**
Strength (MPa)	42.1	43.2	44.2	41.2	**42.7**	39.7	38	41.1	**39.6**
Avg. axial strain	0.01662	0.01281	0.01062	0.01449	**0.01363**	0.01446	0.01212	0.02333	**0.01664**
Avg. hoop strain	0.0063	0.00689	0.0066	0.00443	**0.00606**	0.00671	0.00672	0.0081	**0.00718**

F.D = Freeze-thaw damage

Table 3—Test results of GFRP-wrapped concrete cylinders

FREEZE-THAW

	Under sustained load					No sustained load			
Specimen code	GFS-1	GFS-2	GFS-3	GFS-4	**Avg.**	GFC-1	GFC-2	GFC-3	**Avg.**
Strength (MPa)	38.6	36.7	33.6	37.7	**36.6**	38	32.6	36.4	**35.7**
Avg. axial strain	0.01665	0.01342	0.01523	0.0128	**0.01453**	0.02183	0.01521	0.01777	**0.01827**
Avg. hoop strain	0.01201	0.01611	0.00904	0.0109	**0.01202**	0.02047	0.01145	0.01712	**0.01635**

ROOM TEMPERATURE

	Under sustained load					No sustained load			
Specimen code	GRS-1	GRS-2	GRS-3	GRS-4	**Avg.**	GRC-1	GRC-2	GRC-3	**Avg.**
Strength (MPa)	38.9	37.7	36.9	38.1	**37.9**	38.4	38.5	37.1	**38.0**
Avg. axial strain	0.02045	0.01423	0.01681	0.01378	**0.01632**	0.01545	0.01565	0.0204	**0.01717**
Avg. hoop strain	0.0142	0.01274	0.01344	0.01674	**0.01428**	0.01848	0.01611	0.01567	**0.01675**

Table 4—Test results of unconfined concrete cylinders

ROOM TEMPERATURE

	Dry condition				Wet-dry condition		
Specimen code	URC-1	URC-2	URC-3	**Avg.**	UCWD-1	UCWD-2	**Avg.**
Strength (MPa)	21.9	20.1	21.7	**21.2**	22.5	21.5	**22.0**
Avg. axial strain	0.00175	0.00174	0.0014	**0.00163**	0.00137	0.00236	**0.00186**
Avg. hoop strain	0.00098	0.00036	0.00052	**0.00062**	0.00026	0.00064	**0.00045**

Table 5—Numerical results obtained using ISIS Canada confinement model

CFRP-WRAPPED CYLINDERS

Parameters								Results			Exp.
α_{pc}	N_b	Φ_{frp}	t_{frp} mm	D_g mm	f_{frpu} MPa	Φ_c	f'_c MPa	f_{lfrp} MPa	ω_w	f'_{cc} MPa	f'_{cc} MPa
1	1	1.0	0.89	152	991	1.0	22	7.41	1.12	45.2	39.6

GFRP-WRAPPED CYLINDERS

Parameters								Results			Exp.
α_{pc}	N_b	Φ_{frp}	t_{frp} mm	D_g mm	f_{frpu} MPa	Φ_c	f'_c MPa	f_{lfrp} MPa	ω_w	f'_{cc} MPa	f'_{cc} MPa
1	1	1.0	1.3	152	575	1.0	22	4.71	0.71	41.6	38.0

Table 6—Numerical results obtained using ACI 440 confinement model

CFRP-WRAPPED CYLINDERS

Parameters									Results			Exp.
f'_c MPa	K_a	n	t_f mm	h mm	f_{fe} GPa	C_E	ε^*_{fu}	E_f GPa	ρ_f	f_l MPa	f'_{cc} MPa	f'_{cc} MPa
22	1	1	0.89	153	0.8	1.0	0.01	78.6	0.0232	7.33	55.5	39.6

GFRP-WRAPPED CYLINDERS

Parameters									Results			Exp.
f'_c MPa	K_a	n	t_f mm	h mm	f_{fe} MPa	C_E	ε^*_{fu}	E_f MPa	ρ_f	f_l MPa	f'_{cc} MPa	f'_{cc} MPa
22	1	1	1.3	154	0.4	1.0	0.02	26.1	0.0338	3.79	47.9	38.0

Table 7—Comparison of confinement models

CFRP-wrapped cylinders		
	Strength MPa	% Difference to experimental
Exp.	39.6	
ISIS	45.2	14 %
ACI 440	55.5	40 %

GFRP-wrapped cylinders		
	Strength MPa	% Difference to experimental
Exp.	38.0	
ISIS	41.6	10 %
ACI 440	47.9	26 %

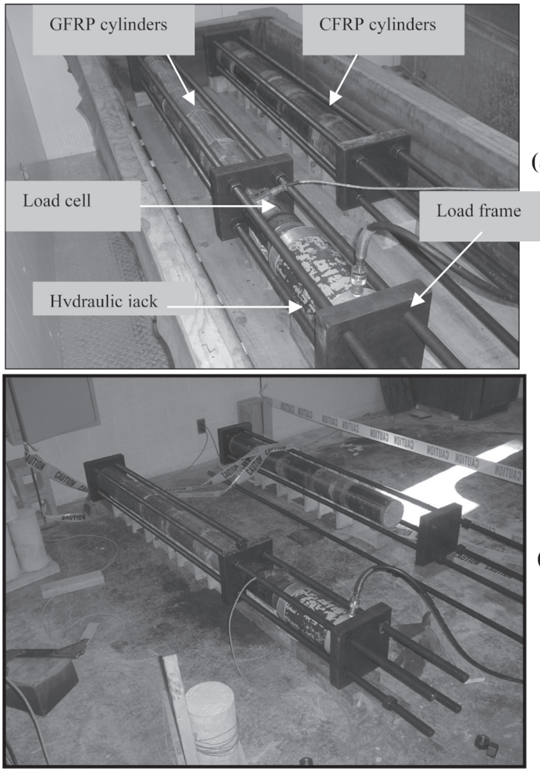

(a) Frames in cold room

(b) Frames at room temperature

Figure 1—Sustained loading frames

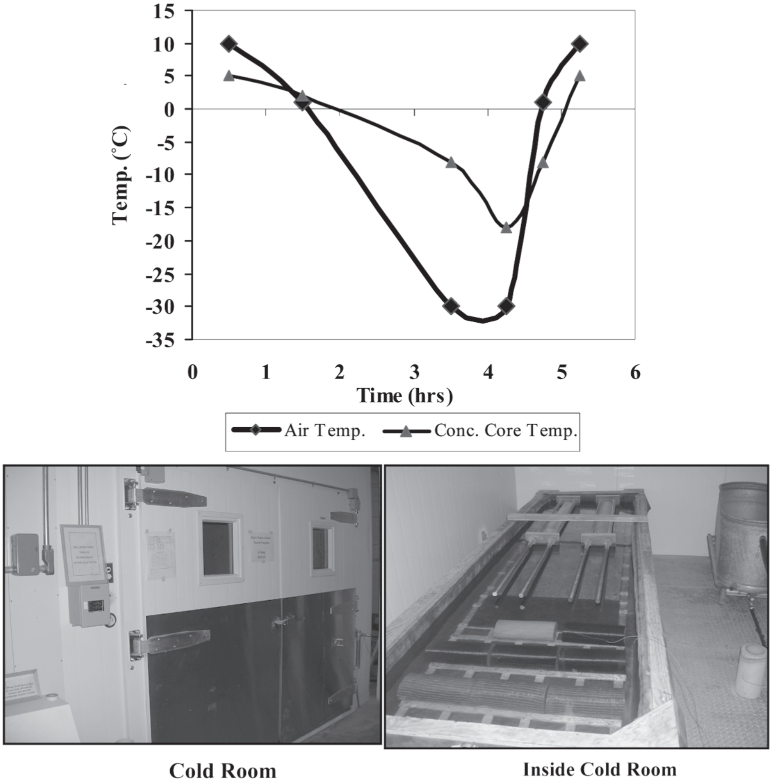

Figure 2—Temperature variation during one complete freeze-thaw cycle inside the cold room, which is also shown

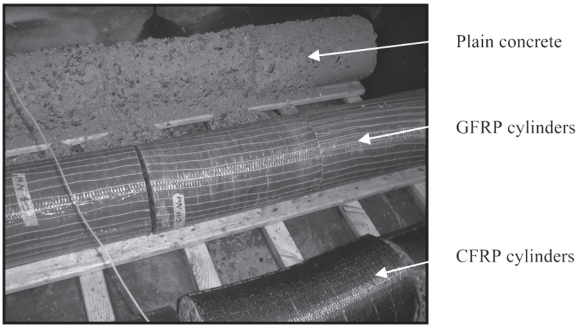

(a)

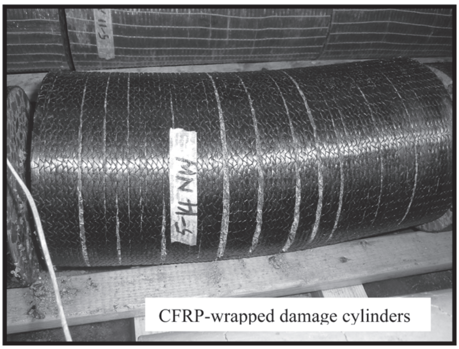

(b)

Figure 3—(a) Unwrapped non-air entrained cylinders disintegrated after 100 freeze-thaw cycles, (b) CFRP-wrapped cylinder without end restraints after 300 freeze-thaw cycles

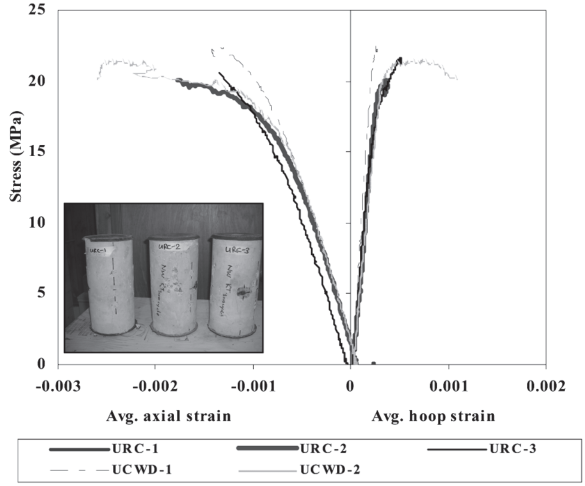

Figure 4—Stress-strain curves for unconfined cylinders at room temperature, URC-dry, UCWD –wet-dry.

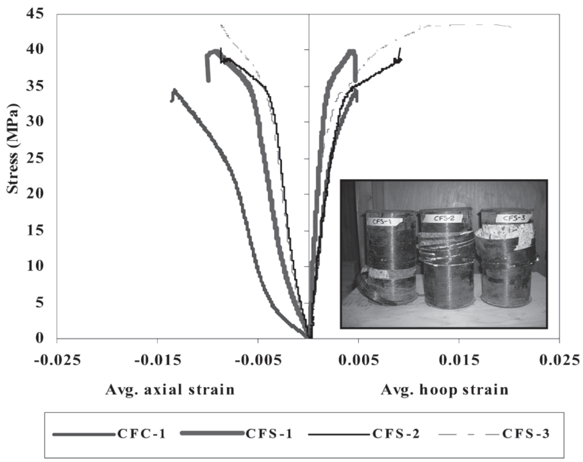

Figure 5—Stress-strain curves for CFRP-wrapped cylinders after 300 freeze-thaw cycles.

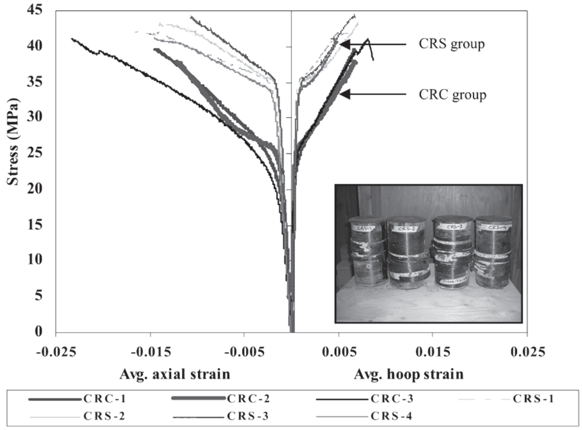

Figure 6—Stress-strain curves for CFRP-wrapped cylinders at room temperature, CRC–no load, CRS–sustained load.

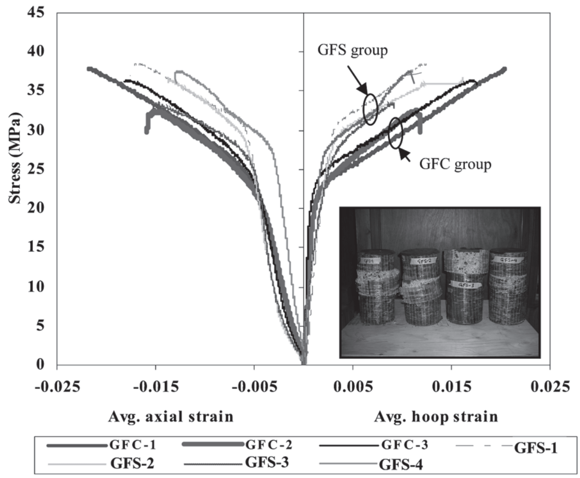

Figure 7—Stress-strain curve for GFRP-wrapped cylinders after 300 freeze-thaw cycles, GFC–no load, GFS–sustained load.

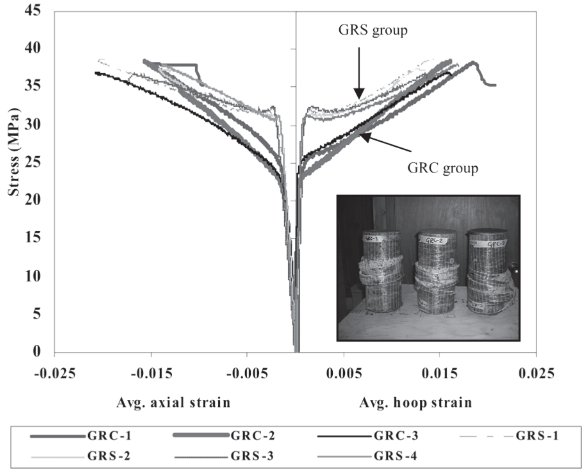

Figure 8—Stress-strain curves for GFRP-wrapped cylinders at room temperature, GRC–no load, GRS–sustained load

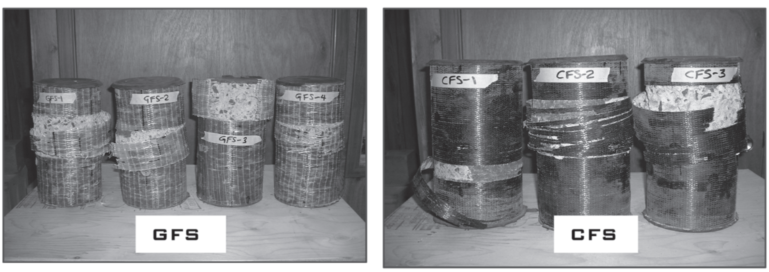

Figure 9—Failure modes of GFRP and CFRP-wrapped specimens tested in compression after freeze-thaw and sustained loading exposure